Cell, Vol. 98, 453–463, August 20, 1999, Copyright ©1999 by Cell Press

The *Drosophila* Caspase Inhibitor DIAP1 Is Essential for Cell Survival and Is Negatively Regulated by HID

Susan L. Wang,* Christine J. Hawkins,* Soon Ji Yoo,* H.-Arno J. Müller,†‡ and Bruce A. Hay*‡
*Division of Biology MC 156-29
California Institute of Technology
Pasadena, California 91125
†Institut für Genetik
Heinrich-Heine Universität Düsseldorf
Universitätsstrasse 1
D-40225 Düsseldorf
Germany

Summary

***Drosophila* Reaper (RPR), Head Involution Defective (HID), and GRIM induce caspase-dependent cell death and physically interact with the cell death inhibitor DIAP1. Here we show that HID blocks DIAP1's ability to inhibit caspase activity and provide evidence suggesting that RPR and GRIM can act similarly. Based on these results, we propose that RPR, HID, and GRIM promote apoptosis by disrupting productive IAP–caspase interactions and that DIAP1 is required to block apoptosis-inducing caspase activity. Supporting this hypothesis, we show that elimination of *DIAP1* function results in global early embryonic cell death and a large increase in DIAP1-inhibitable caspase activity and that *DIAP1* is still required for cell survival when expression of *rpr*, *hid*, and *grim* is eliminated.**

Introduction

Programmed cell death, or apoptosis, is an evolutionarily conserved process by which organisms remove damaged or unwanted cells (reviewed in Wyllie et al., 1980; Raff, 1992). Central components of the machinery that carries out this process are caspases, a family of aspartate-specific, cysteine-dependent proteases (Alnemri et al., 1996). Caspases are made as zymogens, comprising three functional modules: a prodomain and two catalytic subunits known as the large, or p20, and the small, or p10, subunits. In general, caspases are activated in vivo following cleavage at aspartate residues that separate the prodomain from the catalytic region and separate the large and small subunits of the catalytic domain. The aspartates cleaved in caspase zymogens often resemble consensus target sites of known caspases. This has suggested that caspases may function in a cascade in which initiator caspases, activated by upstream death signals, cleave and activate a set of executioner caspases that carry out proteolytic cleavages of cellular proteins, leading ultimately to cell death (reviewed in Nicholson and Thornberry, 1997; Salvesen and Dixit, 1997; Cryns and Yuan, 1998; Thornberry and Lazebnik, 1998).

‡To whom correspondence should be addressed (e-mail: muellear@uni-duesseldorf.de [H.-A. J. M.], haybruce@its.caltech.edu [B. A. H.]).

Because caspases have the potential to initiate cascades of proteolysis, it is important that their activity be tightly regulated. The only cellular caspase inhibitors identified to date all share homology with a family of cell death inhibitors identified in baculoviruses, known as inhibitors of apoptosis, or IAPs (Crook et al., 1993; Birnbaum et al., 1994; reviewed in LaCasse et al., 1998 and Deveraux and Reed, 1999). IAP homologous proteins have been identified in other viruses, *Drosophila melanogaster*, *Caenorhabditis elegans*, mammals, and yeast (reviewed in Uren et al., 1998). These proteins are characterized by one or more N-terminal repeats of a motif known as the baculovirus IAP repeat (BIR). Many also have a C-terminal RING finger motif. Some IAP homologous proteins have been shown to act as cell death inhibitors. In several cases, this activity is localized to the BIR-containing region of the protein (reviewed in LaCasse et al., 1998; Uren et al., 1998; Deveraux and Reed, 1999), which has also been shown to mediate caspase binding and inhibition (Deveraux et al., 1997, 1998; Roy et al., 1997; Takahashi et al., 1998; Hawkins et al., 1999).

Proteins that initiate cell death by disrupting IAP–caspase interactions have not been described. However, the products of the *Drosophila reaper* (*rpr*), *head involution defective* (*hid*), and *grim* genes are interesting candidates. All three loci are located in the 75C region of the *Drosophila* genome, and deletion of this region eliminates death induced by many different stimuli, indicating that important cell death activators reside within (White et al., 1994). Furthermore, individual overexpression of any one of these genes is sufficient to initiate caspase-dependent cell death in many cells that normally live (Grether et al., 1995; Hay et al., 1995; Chen et al., 1996; White et al., 1996; Vucic et al., 1997, 1998; Zhou et al., 1997; Wing et al., 1998). Two *Drosophila* IAPs, DIAP1, the product of the *thread* (*th*) locus (Hay et al., 1995), and DIAP2 (Hay et al., 1995; Duckett et al., 1996; Uren et al., 1996), suppress *rpr*-, *hid*-, and *grim*-dependent cell death when overexpressed (Hay et al., 1995; Vucic et al., 1997, 1998; Bergmann et al., 1998; Wing et al., 1998), and DIAP1 and DIAP2 can immunoprecipitate RPR, HID, and GRIM from insect cells (Vucic et al., 1997, 1998). Furthermore, DIAP1 binds a processed form of the caspase drICE in insect cells (Kaiser et al., 1998) and inhibits the activity of a second caspase, DCP-1 (Hawkins et al., 1999). These observations suggest several models of how *Drosophila* IAPs, RPR, HID, GRIM, and *Drosophila* caspases might interact to regulate cell death (Kaiser et al., 1998). In one model, RPR, HID, or GRIM activates caspases through an IAP-independent pathway. In this model, *Drosophila* IAPs suppress apoptosis by acting as a sink for these proteins and by inhibiting caspase activation or activity initiated by their action. In a second model, DIAP1 functions primarily as a caspase inhibitor, and RPR, HID, and/or GRIM initiate caspase-dependent cell death by preventing IAPs from productively interacting with caspases.

The yeast *Saccharomyces cerevisiae* provides an

ideal system to study interactions between caspases and molecules that regulate their activity (Hawkins et al., 1999; Kang et al., 1999). While yeast cells do not exhibit apoptosis, and database searches have failed to uncover yeast homologs of the core apoptosis regulators identified in worms, flies, and mammals, overexpression of DCP-1 or drICE results in yeast cell death that is blocked by DIAP1. Here we used yeast expressing these proteins as a system to assay the ability of RPR, HID, and GRIM to disrupt IAP–caspase interactions. We found that all three proteins, while nontoxic on their own, killed yeast coexpressing DCP-1 or drICE and DIAP1, suggesting that they were blocking DIAP1's ability to function as a caspase inhibitor. We pursued the basis for this activity further with HID and found, both in yeast and in vitro, that proteins containing the N-terminal 37 residues of HID, which are sufficient to induce apoptosis in insect cells (Vucic et al., 1998), suppressed DIAP1's ability to inhibit DCP-1 activity. We also found that the *DIAP1* loss-of-function phenotype consists of an embryo-wide set of cellular changes reminiscent of apoptotic cell death and that these were associated with the activation of DIAP1-inhibitable caspase activity. Furthermore, double mutants that remove zygotic *rpr*, *hid*, *grim*, and *DIAP1* function showed phenotypes similar to those of the *DIAP1* loss-of-function mutant alone. These observations suggest that a principal function of DIAP1 is to promote cell survival by blocking caspase activity and that at least one mechanism by which RPR, HID, and GRIM promote apoptosis is by disrupting IAP–caspase interactions.

Results and Discussion

RPR, HID, and GRIM Block DIAP1's Ability to Suppress Caspase-Dependent Cell Death in Yeast

Yeast were transformed with two plasmids: one in which DCP-1 expression was driven by the inducible GAL1 promoter, and a second in which DIAP1 expression was driven by the constitutive Adh promoter (hereafter referred to as DCP-1-DIAP1 yeast). These cells were then transformed with a second GAL1 expression plasmid that was either an empty vector or carried GAL1-driven RPR, HID, or GRIM. Transformants were spotted as a series of 10-fold serial dilutions onto glucose plates to indicate the number of cells and onto galactose plates to induce expression of DCP-1 and RPR, HID, or GRIM. DCP-1-DIAP1 yeast carrying an empty vector survived on galactose, but DCP-1-DIAP1 yeast expressing HID or GRIM did not (Figure 1A). Expression of RPR under GAL1 control did not kill DCP-1-DIAP1 yeast in which DIAP1 expression was driven by the Adh promoter, but it was able to kill DCP-1-DIAP1 yeast in which DIAP1 expression was driven by a weaker promoter, the copper-inducible CUP1 promoter, in the presence of 30 μM Cu^{2+} (Figure 1A). Importantly, expression in yeast of RPR, HID, or GRIM alone under GAL1 control had no effect on cell growth as compared with yeast expressing only the empty vector (Figure 1A). These results suggest that RPR, HID, and GRIM are able to block DIAP1's ability to inhibit DCP-1 caspase activity.

Three other *Drosophila* caspases, drICE, DCP-2/Dredd, and DRONC, have been implicated as effectors of apoptosis (Fraser and Evan, 1997; Fraser et al., 1997; Chen et al., 1998; Dorstyn et al., 1999). We wanted to determine if RPR, HID, and GRIM played a similar role in regulating their activity. We focused our attention on drICE. A version of drICE lacking the prodomain is not inhibited by DIAP1 (Hawkins et al., 1999), but a version of drICE that contains prodomain sequences is (C. J. H. and B. A. H., unpublished observations). Full-length drICE expressed in yeast under GAL1 control neither kills nor activates a cleavage-dependent reporter, probably because the caspase does not significantly autoactivate (Hawkins et al., 1999). We created a form of drICE that is active in yeast and contains prodomain sequences by generating a "reversed" form of drICE, rev-drICE, in which the drICE p10 domain was placed N-terminal to prodomain and p20 sequences (Figure 1B). Reversed forms of mammalian caspases that are not otherwise active are constitutively active (Srinivasula et al., 1998). As shown in Figure 1B, expression of rev-drICE under GAL1 control kills yeast, and this death is prevented by coexpression of DIAP1. Importantly, as with DCP-1, expression of HID, GRIM, or RPR killed yeast coexpressing rev-drICE and DIAP1.

The N Terminus of HID Mediates Its Ability to Disrupt IAP–Caspase Interactions in Yeast

In insect cells, the N-terminal 37 amino acids of HID, expressed in the context of a larger fusion protein, are necessary and sufficient to induce apoptosis and to mediate HID's binding to DIAP1 (Vucic et al., 1998). To test the activity of these sequences in yeast, we generated GAL1 expression constructs similar to those of Vucic et al. (1998) in which the first 37 amino acids of HID were either present or absent (Figure 1C). HIDΔ(38–335) encodes a protein in which the first 37 amino acids of HID are fused to the C-terminal 74; HIDΔ(1–335) consists of only the last 74 residues of HID; and HIDΔ(1–36) encodes a protein that lacks the first 36 residues of HID but contains the rest of the full-length HID coding sequence. GAL1-dependent expression of HIDΔ(38–335) in DCP-1-DIAP1 yeast resulted in no growth. In contrast, DCP-1-DIAP1 yeast expressing HIDΔ(1–335) grew normally. HIDΔ(1–36) had weak killing activity in this assay (Figure 1D) but not in insect cell death assays (Vucic et al., 1998) or other in vitro assays described below. As with full-length HID, expression of HIDΔ(38–335), HIDΔ(1–335), or HIDΔ(1–36) in isolation had no effect on yeast cell growth (Figure 1D). Thus, proteins carrying the N-terminal 37 residues of HID, which are sufficient to kill insect cells, are also able to kill DCP-1-DIAP1 yeast.

HID Suppresses DIAP1's Ability to Inhibit DCP-1 Caspase Activity In Vitro

The results of our yeast experiments suggested that HID directly inhibits DIAP1. We tested this idea in vitro using purified proteins. Bacterially expressed and purified versions of DCP-1, DIAP1, and HID (Figure 2A) were mixed in various combinations and DCP-1 caspase activity measured fluorometrically (Figures 2B and 2C). His6-tagged DCP-1 (DCP-1-His6) is active as a caspase, and this activity was inhibited by DIAP1 but not GST

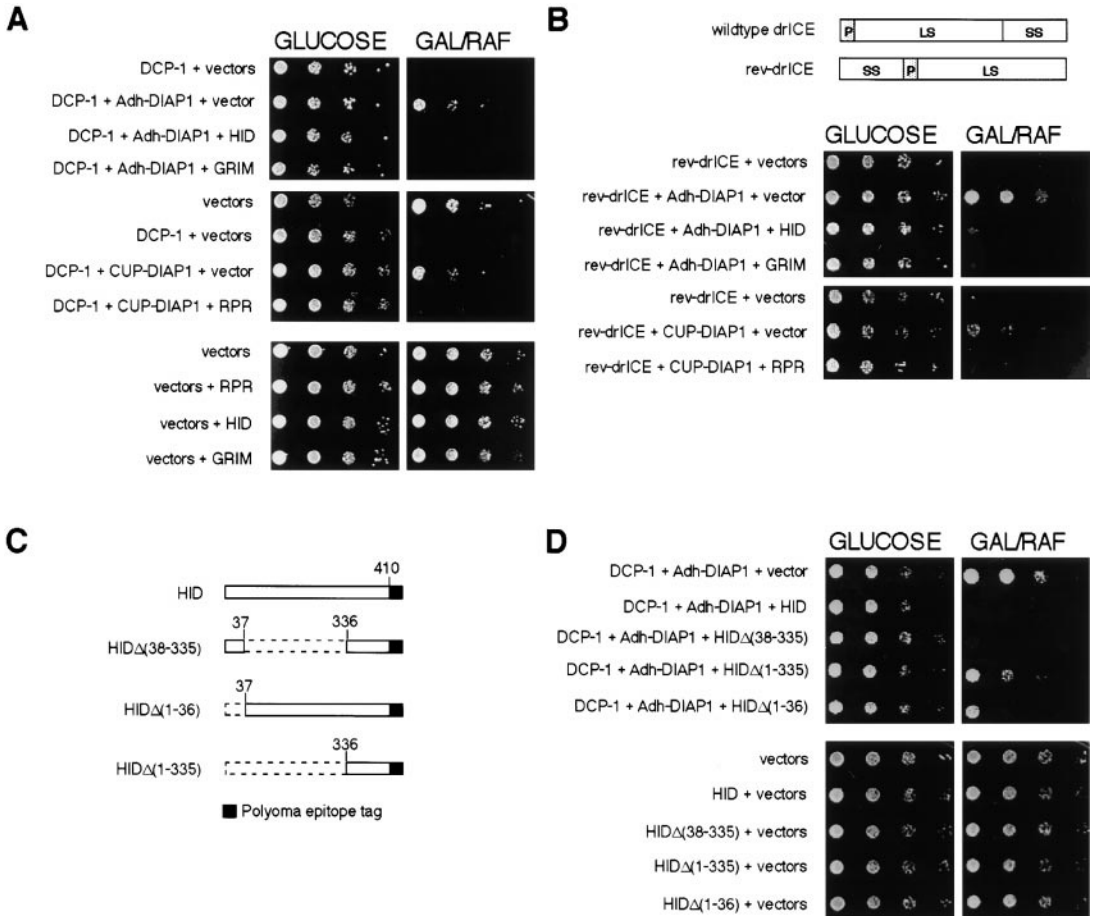

Figure 1. RPR, HID, and GRIM Block DIAP1's Ability to Suppress Caspase-Dependent Yeast Cell Death

(A) RPR, HID, and GRIM kill yeast expressing DCP-1 and DIAP1. Top: GAL1-driven DCP-1 causes yeast cell death that is prevented by Adh-dependent expression of DIAP1 (DCP-1 + Adh-DIAP1 + vector). GAL1-driven HID (DCP-1 + Adh-DIAP1 + HID) or GRIM (DCP-1 + Adh-DIAP1 + GRIM) results in yeast cell death. Middle: GAL1-driven RPR kills yeast expressing DCP-1 and CUP1-driven DIAP1 (DCP-1 + CUP-DIAP1 + RPR) in the presence of 30 μM Cu^{2+}. Bottom: Expression of RPR, HID, or GRIM in the presence of empty vectors does not affect yeast cell viability.

(B) RPR, HID, and GRIM kill yeast expressing rev-drICE and DIAP1. Top: drICE contains prodomain (P), large (LS), and small (SS) subunits. In reversed drICE (rev-drICE), the predicted drICE small subunit was placed N-terminal to drICE prodomain and large subunit sequences. Middle: Expression of HID or GRIM kills yeast expressing rev-drICE and Adh-DIAP1 (rev-drICE + Adh-DIAP1 + HID; rev-drICE + Adh-DIAP1 + GRIM). Bottom: Expression of RPR kills yeast expressing rev-drICE and CUP-DIAP1 (rev-drICE + CUP-DIAP1 + RPR) in the presence of no added Cu^{2+}.

(C) Diagram of HID constructs. Numbers represent amino acid positions in full-length HID. Solid lines indicate regions of HID present in the fusion protein; dashed lines indicate sequences that are deleted. A polyoma epitope tag present at the C terminus of each coding region is indicated by a black bar.

(D) Proteins containing the first 37 residues of HID block DIAP1's ability to inhibit DCP-1 activity in yeast. Top: Effects of expression of HID fusion proteins on the viability of DCP-1 + Adh-DIAP1 yeast. Bottom: Effects of expression of HID fusion proteins and empty vectors on yeast viability.

(Hawkins et al., 1999; Figure 2B). Addition of HID alone to a reaction containing DCP-1-His6 did not alter DCP-1-His6 activity, indicating that HID has no direct effect on DCP-1-His6 (Figure 2B). However, when full-length HID was incubated with DIAP1 and DCP-1-His6, DIAP1-dependent inhibition of DCP-1-His6 activity was lost (Figure 2B). Incubation of DIAP1 and DCP-1-His6 with HIDΔ(1–36)-His6 had little or no effect on DIAP1's ability to inhibit DCP-1-His6 activity, indicating that the first 37 residues of HID are necessary for this activity. To determine if the first 37 residues of HID were sufficient to mediate this effect, we carried out experiments using a version of HID that consists of the first 37 residues of HID fused to GST and a C-terminal His6 tag [HID(1–37)GST-His6]. As shown in Figure 2C, addition of HID(1–37)GST-His6 to an assay containing DCP-1-His6 and DIAP1 blocked DIAP1's ability to inhibit DCP-1-His6 activity, while addition of an equivalent amount of GST-His6 had no effect. Thus, consistent with our observations in yeast, purified HID directly blocks DIAP1's ability to inhibit DCP-1 caspase activity, and the first 37 amino acids of HID, at least in the context of a larger fusion protein, are necessary and sufficient for this activity.

To determine if HID directly interacts with DIAP1 or DCP-1, we carried out binding experiments. As expected from the results of our yeast and in vitro activity

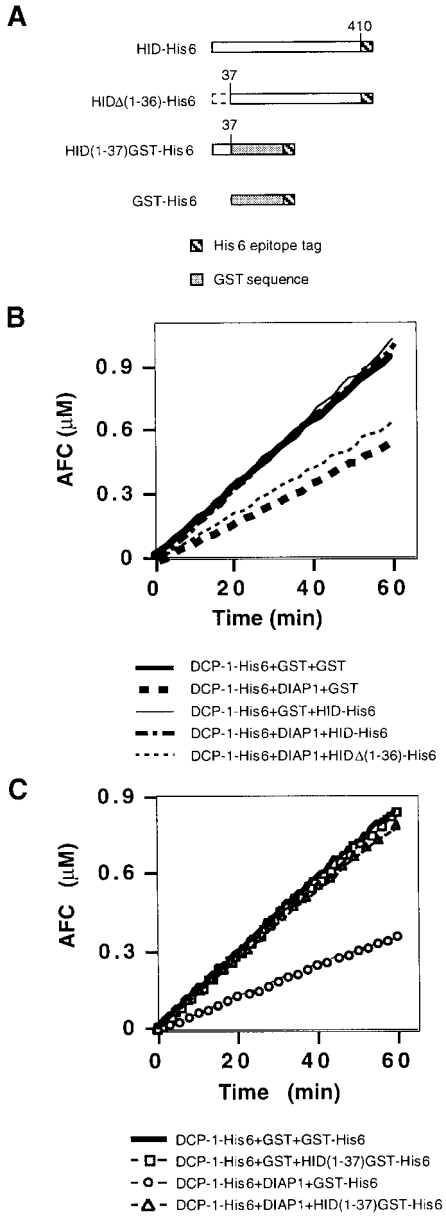

Figure 2. Proteins Containing the First 37 Residues of HID Block DIAP1's Ability to Inhibit DCP-1 Activity In Vitro

(A) Schematic of HID constructs. HID coding regions are represented by open boxes and deleted regions by dashed lines.

(B) The N-terminal 36 residues of HID are required to inhibit DIAP1 function. DCP-1-His6 (0.2 nM) activity was measured by following the release of AFC fluorometrically from the Ac-DEVD-AFC substrate over time. The total protein concentration in each incubation was kept constant, with GST (0.2 μM or 0.77 μM) being used to replace DIAP1 (0.2 μM), HID-His6 (0.44 μM), or HIDΔ(1–36)-His6 (0.44 μM) as the assay required.

(C) A protein containing the N-terminal 37 residues of HID, HID(1–37)GST-His6, is sufficient to block DIAP1's caspase inhibitory activity. Assays were performed as in (B).

assays, GST-DIAP1 coupled to glutathione–Sepharose bound full-length HID-His6 and DCP-1-His6 but did not appreciably bind HIDΔ(1–36)-His6. GST alone showed no interaction with any of these proteins (Figure 3A). Also, a maltose-binding protein–DIAP1 fusion protein

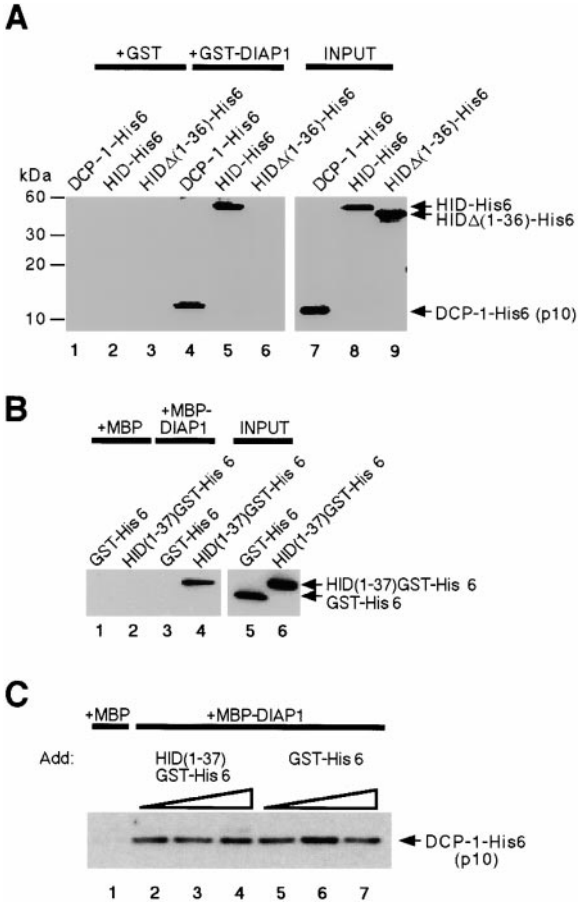

Figure 3. Physical Interactions between HID, DIAP1, and DCP-1

(A) DIAP1 binds DCP-1 and HID, and the first 37 residues of HID are required for this interaction. Glutathione-Sepharose-bound GST or GST-DIAP1 was incubated in binding buffer with DCP-1-His6, HID-His6, or HIDΔ(1–36)-His6 (Figure 2A). Binding reactions were followed by washes and Western blotting. A fraction of the input of DCP-1-His6, HID-His6, and HIDΔ(1–36)-His6 is shown.

(B) DIAP1 binds proteins containing only the first 37 residues of HID. Amylose resin–bound MBP or MBP-DIAP1 was incubated with GST-His6 or HID(1–37)GST-His6 and processed as above.

(C) HID(1–37)GST-His6 does not prevent DCP-1-His6 from binding MBP-DIAP1. MBP-DIAP1 bound to amylose resin was incubated with increasing amounts of HID(1–37)GST-His6 or GST-His6. Following this preincubation, a constant amount of DCP-1-His6 was introduced into the mixture. The beads were washed and processed for Western blotting using an anti-His antibody to detect DCP-1-His6. MBP beads incubated with the highest concentration of HID(1–37)GST-His6 and equivalent amounts of DCP-1-His6 were processed in a similar manner.

(MBP-DIAP1) bound to amylose resin was able to bind HID(1–37)GST-His6, while MBP bound to the same resin was not (Figure 3B). Furthermore, HID(1–37)GST-His6, bound to glutathione–Sepharose beads, was able to bind ^{35}S-methionine-labeled, in vitro–translated DIAP1 but not in vitro–translated DCP-1 (data not shown). These observations, in conjunction with the fact that HID-His6 or HID(1–37)GST-His6 alone had no effect on DCP-1-His6 caspase activity (Figures 2B and 2C), suggest that HID's effects on caspase activity are mediated through DIAP1.

To explore the mechanism by which HID blocks DIAP1's ability to inhibit DCP-1, we asked if HID(1–37)GST-His6 was able to displace DCP-1-His6 from DIAP1. MBP-DIAP1 bound to amylose resin was preincubated with increasing amounts of GST or HID(1–37)GST-His6 followed by addition of DCP-1-His6. Binding reactions were followed by washes and analysis of the bead-bound proteins by Western blotting. As shown in Figure 3C, DCP-1 binding to MBP-DIAP1 was not appreciably decreased by the presence of up to a 20-fold molar excess of GST-His6 or HID(1–37)GST-His6 over MBP-DIAP1. As expected, MBP beads incubated with HID(1–37)GST-His6 showed no binding to DCP-1-His6. Thus, we see no evidence that HID(1–37)GST-His6, at molar ratios with respect to DIAP1 greater than those used to demonstrate inhibition of DIAP1 function in caspase activity assays (Figure 2C), prevents binding of DCP-1-His6 to MBP-DIAP1. These observations suggest that HID(1–37)GST-His6 does not prevent DIAP1 from inhibiting DCP-1 activity by blocking DCP-1 binding. It is important to note, however, that full-length HID, which has a large C-terminal domain that can regulate HID activity (Bergmann et al., 1998), may behave differently.

Our observations suggest that RPR, HID, and GRIM can promote caspase-dependent cell death by blocking DIAP1's ability to inhibit caspase activity. These conclusions are supported by the observations that in insect cells, RPR, HID, and GRIM promote caspase-dependent cell death that is sensitive to the levels of DIAP1 (Hay et al., 1995; Vucic et al., 1997, 1998; Bergmann et al., 1998; Wing et al., 1998), that these proteins associate with DIAP1 in vivo (Vucic et al., 1997, 1998), and that DIAP1 binds and inhibits caspases (Kaiser et al., 1998; Hawkins et al., 1999; this work). Furthermore, since proteins that contain only the first 37 amino acids of HID are sufficient to initiate the caspase-dependent death of insect cells and to block DIAP1's ability to inhibit caspase activity, but other regions of HID lack activity in insect cells, it is likely that disrupting DIAP1's ability to inhibit caspase activity is an important mechanism by which HID promotes cell death. Because of difficulties with solubility of RPR and GRIM under conditions that allowed productive DIAP1–caspase interactions, we were unable to carry out in vitro experiments similar to those carried out with HID. However, based on the fact that they behaved similarly to HID in yeast expressing DCP-1 or rev-drICE and DIAP1, it seems likely that they also are able to block DIAP1's ability to inhibit caspase activity.

Our observations do not exclude the possibility that RPR, HID, and GRIM promote apoptosis through other pathways as well. For example, RPR has been shown to promote apoptosis in a *Xenopus laevis* system (Evans et al., 1997) through association with a novel protein, SCYTHE (Thress et al., 1998), and peptides corresponding to N-terminal sequences of RPR and GRIM block K^+ channel function (Avdonin et al., 1998). Furthermore, as described below, removal of DIAP1 in the embryo results in massive cell death, but the *DIAP1* mutant cells do not show all the features of apoptosis seen in wild-type embryos, consistent with the idea that other pathways may be necessary to create a complete apoptotic response.

DIAP1 Mutant Embryos Show Global Early Morphogenetic Arrest and Cell Death Associated with an Increase in DIAP1-Inhibitable Caspase Activity

If disruption of IAP–caspase interactions is an important mechanism by which cell death is initiated in *Drosophila*, then caspase activity must be continually held in check by DIAP1 and/or other IAPs in order to block an ever-present death signal. To explore this possibility, we characterized the embryonic phenotype of mutations (alleles of *th*) that disrupt *DIAP1* function.

Homozygous *th* mutant embryos exhibit a severe terminal embryonic lethal phenotype and do not form a cuticle (Figure 4G and data not shown). We monitored early development of loss-of-function *th* embryos from th^5, a strong loss-of-function allele, and a deficiency for the region, *Df(L)brm11* (Figure 4). th^5 and *Df(3R)brm11* homozygous embryos undergo normal cellularization and initial gastrulation movements such as ventral furrow formation, cephalic furrow formation, and posterior midgut invagination (Figures 4A–4C). However, during germband extension, within 15 to 30 min after the onset of gastrulation movements, virtually all morphogenetic movements cease (Figures 4A–4C). While the stage of initial arrest is somewhat variable in time (compare Figures 4B and 4C with respect to the extent of ventral furrow formation and posterior midgut invagination), within the next hour all the cells adopt a rounded morphology and the yolk cell fragments and eventually moves to the surface of the embryo. The disruption of embryonic integrity is seen particularly clearly in Figures 4D–4G, in which wild-type and th^5 mutant embryos are visualized using scanning electron microscopy. While some th^5 homozygous embryos showed normal morphology at the beginning of germband extension (data not shown), other embryos with a similar degree of extension movements showed extensive cell rounding, suggesting a disruption of intercellular adhesion (Figures 4D and 4E). All th^5 embryos also show a regression of the cephalic furrow (compare Figure 4A with Figures 4B and 4C, and Figure 4D with 4E). At the extended germband stage (stage 9), the surface of cells in control embryos is smooth and the cells are closely apposed to each other (Figure 4F). In contrast, by this time th^5 homozygotes have adopted a uniform cellular morphology in which all cells have a round shape, the surface of the cells contains many membrane blebs, and vesicular cell fragments similar to those seen in dying cells are present (Figure 4G). The yolk cell, normally located interiorly, is visible at the surface. Thus, zygotic loss of *DIAP1* function results in early morphogenetic arrest followed by severe morphological abnormalities at the beginning of germband extension.

We used TUNEL labeling to determine whether the massive DNA fragmentation characteristic of cells undergoing apoptosis had occurred in cells of *th* mutants (Figure 5). Wild-type embryos during germband extension showed significant DNA fragmentation in only a few cells (Figures 5A, 5C, and 5E). In contrast, comparably staged th^5 embryos labeled extensively in most if not all cells. Initially, the TUNEL signal is relatively weak (Figures 5B and 5D), but the intensity increases within the following hour of development to a strong uniform labeling (Figures 5B, 5D, and 5F). In contrast,

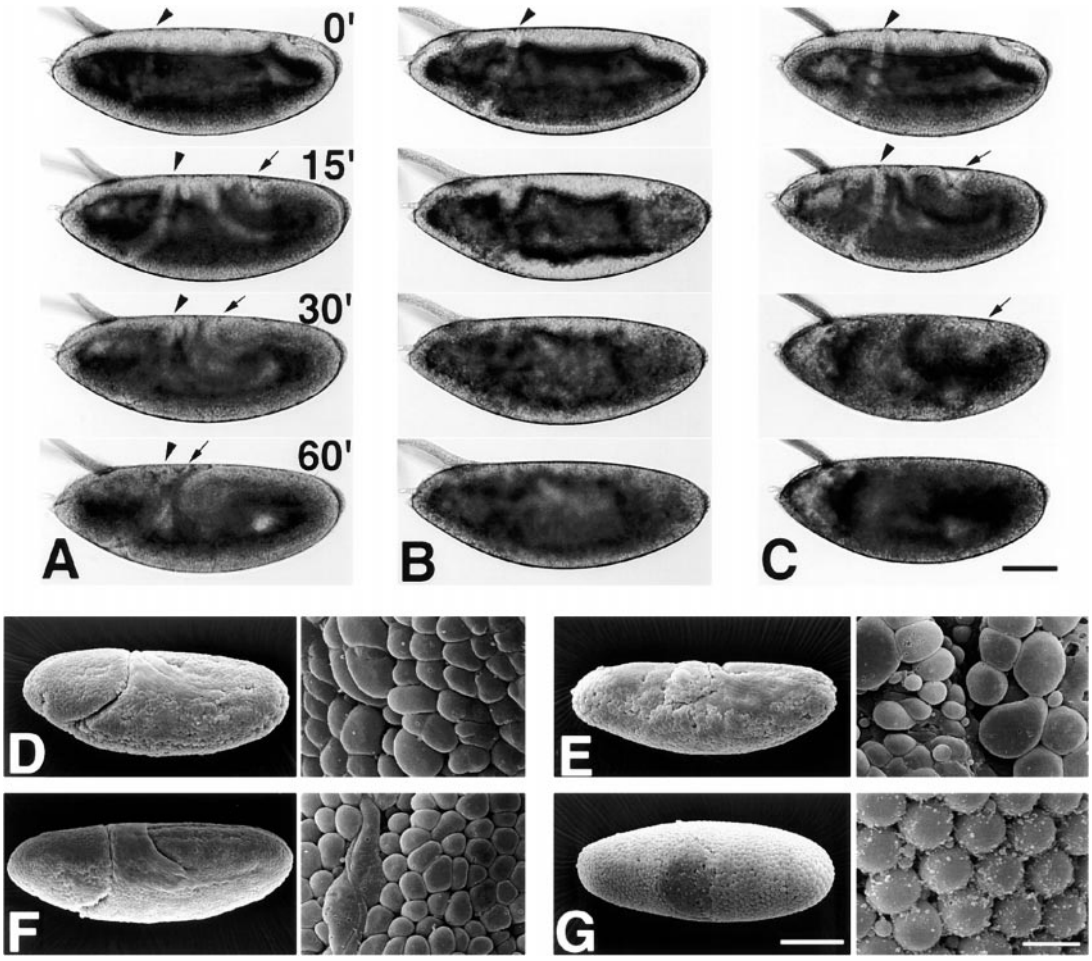

Figure 4. Removal of Zygotic DIAP1 Leads to Morphogenetic Arrest during Germband Extension and Global Cell Shape Changes

(A) Wild-type developmental series of living embryos derived from a *th*^{5}/TM3[ftz::lacZ] stock during gastrulation and germband extension (stages 6 through 9). Arrowheads mark the position of the cephalic furrow, and arrows indicate the front of the extending germband.

(B and C) *th*^{5} and *Df(3L)brm11* homozygous embryos, respectively, at the same developmental stages as in (A).

(D and F) Scanning electron micrographs of balancer-bearing embryos from *th*^{5}/TM3[ftz::lacZ] stock. The right-hand panels show higher magnification of the general morphology of the embryonic surface. (D) shows an embryo at stage 8, and (F) shows an embryo at stage 9.

(E and G) Similarly staged embryos homozygous for *th*^{5}.

Scale bars are 100 μm in (C) and (G) (left-hand panel) and 10 μm in (G) (right-hand panel).

embryos homozygous for the weaker allele *th*^{6} do not show a significant increase in TUNEL-positive cells as compared to comparably staged control embryos at the retracted germband stage (stage 14; Figures 5G and 5H).

To determine if loss of *DIAP1* in fact results in an increase in caspase activity, we measured caspase activity in extracts of 3- to 5-hr-old embryos from wild-type, *th*^{5}, and *th*^{6} stocks by following the release of Ac-DEVD-AFC fluorometrically (Figure 5I). Extracts from wild-type and *th*^{6} embryos had very low levels of caspase activity. In contrast, extracts from *th*^{5} embryos had very large amounts of caspase activity. Importantly, the increased caspase activity present in the *th*^{5} embryonic extracts was inhibited by the addition of purified DIAP1 (Figure 5I), consistent with the idea that DIAP1 normally represses these caspases.

The caspase targets of DIAP1 in the *Drosophila* embryo or other tissues have not been identified. Five caspases have been identified in *Drosophila*: DCP-1 (Song et al., 1997), drICE (Fraser and Evan, 1997), DCP-2/Dredd (Inohara et al., 1997; Chen et al., 1998), DRONC (Dorstyn et al., 1999), and a fifth gene (C. J. H. and B. A. H., unpublished). DIAP1 is able to inhibit the activity of the three caspases we have tested: DCP-1 (Hawkins et al., 1999), drICE (this report), and DRONC (C. J. H., unpublished). The *DIAP1* loss-of-function embryonic phenotype may result from the unrestrained activity of zygotically expressed versions of these caspases. Alternatively, DIAP1 may also function in the early embryo to block the activity of caspases introduced late during oogenesis into the developing oocyte from the degenerating nurse cells (Cavaliere et al., 1998; Chen et al., 1998; Foley and Cooley, 1998; McCall and Steller, 1998; Dorstyn et al., 1999).

DIAP1 Loss-of-Function Mutant Embryos Do Not Stain with Acridine Orange, a Marker of Apoptotic Cell Death

Acridine orange (AO) is commonly used as a marker for apoptotic cell death. It appears to enter all cells but is

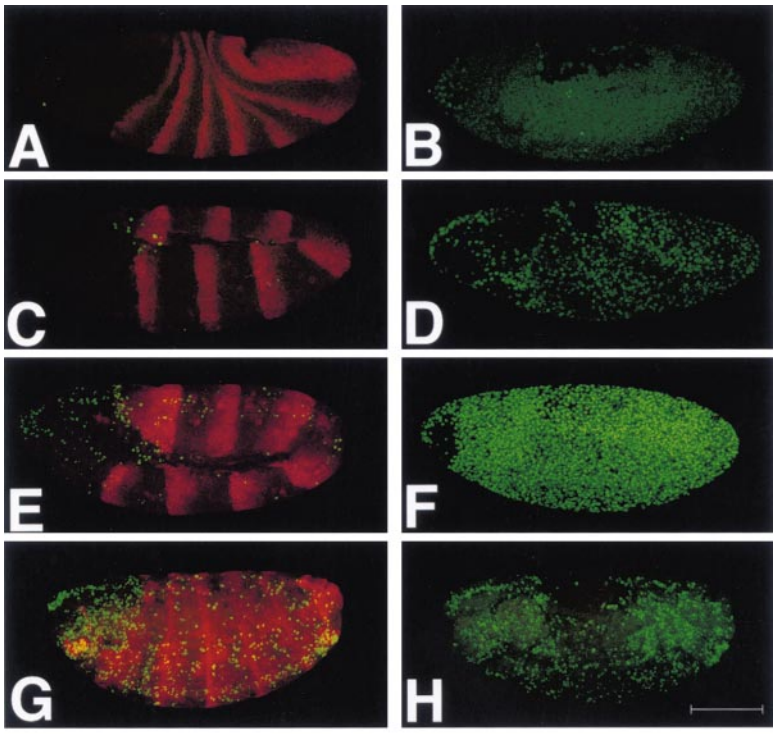

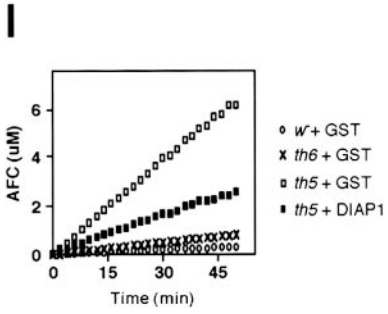

Figure 5. Cells in Embryos Homozygous Mutant for DIAP1 Show Premature and Increased DNA Fragmentation and an Increase in DIAP1-Inhibitable Caspase Activity

(A–F) Confocal images of staged embryos from stocks of th^5/TM3[ftz::lacZ] and (G and H)th^6/TM3[ftz::lacZ] double labeled for TUNEL (green) and β-galactosidase (red). Scale bar is 100 μm. (A) th^5/TM3[ftz::lacZ] and (B) th^5/th^5 embryos at early germband extension (stage 8). (C) th^5/TM3[ftz::lacZ] and (D) th^5/th^5 embryos at extended germband stage (early stage 9). (E) th^5/TM3[ftz::lacZ] and (F) th^5/th^5 embryos at extended germband stage (late stage 9). (G) th^6/TM3[ftz::lacZ] and (H) th^6/th^6 embryos at retracted germband stage (stage 14). (I) Caspase activity of wild-type and *th* mutant embryo extracts in the presence of GST or DIAP1. One microgram of extract of 3- to 5-hr-old embryos from stocks of w^-, th^5/TM3, or th^6/TM3 was introduced into caspase activity buffer containing 100 μM of the Ac-DEVD-AFC substrate and 0.5 μg of either GST or DIAP1. Release of AFC was monitored fluorometrically over time.

only retained (through unknown mechanisms) by cells undergoing apoptosis (see Abrams et al., 1993). In light of the strong defects in *th* mutant embryos reported here, we repeated experiments described in Hay et al. (1995) reporting that *th* embryos did not show an increase in AO staining. Figure 6A shows a bright-field image of a stage 14 th^5/*TM3* embryo. Figure 6B shows the same embryo stained with AO. Dying cells show bright green fluorescence, and living cells do not stain. A th^5 homozygous embryo displaying the *th* terminal phenotype is shown in Figure 6C. All cells have rounded up, and the yolk sac has moved to the surface. However, as shown in Figure 6D, no AO staining is seen despite the fact that embryos at this stage show cell rounding, membrane blebbing, increased caspase activity, and DNA fragmentation. Thus, the *th* phenotype, while showing some features of apoptosis, lacks others. One explanation for this is that the early embryo simply lacks the cellular machinery required to carry out apoptotic steps leading to AO retention. A second possibility is that the

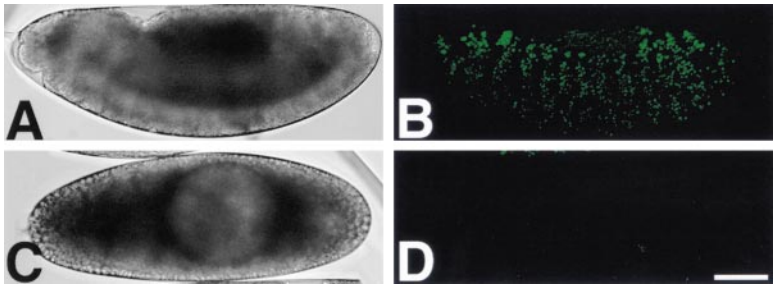

Figure 6. Cells in DIAP1 Loss-of-Function Embryos Do Not Show an Increase in Acridine Orange Staining Characteristic of Cells Undergoing Apoptosis in Wild-Type Embryos

(A and B) stage 14 th^5/TM3[ftz::lacZ] or TM3[ftz::lacZ]/TM3[ftz::lacZ] embryo stained with acridine orange and viewed under the confocal microscope using Nomarski (A) and fluorescence channels (B).

(C and D) th^5 homozygous embryo exhibiting the terminal phenotype. At this stage, acridine orange staining is never observed in th^5 homozygotes (D). Scale bar is 50 μm.

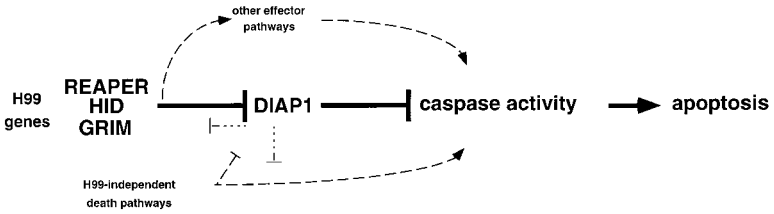

Figure 7. Model for How DIAP1 Regulates Apoptosis

DIAP1 inhibits caspase activity and is essential for cell survival. DIAP1's ability to inhibit caspase activity is suppressed by RPR, HID, and GRIM, thus promoting caspase-dependent cell death. RPR and GRIM have other activities (Evans et al., 1997; Avdonin et al., 1998; Thress et al., 1998), suggesting that these proteins may also promote apoptosis through other pathways. Free DIAP1 may inhibit apoptosis by binding these proteins, sequestering them from their targets. Thus, DIAP1 may act both upstream and downstream of RPR, HID, and GRIM to prevent cell death. Genes within the H99 interval are not required for some cell deaths (White et al., 1994; Foley and Cooley, 1998), indicating that other death pathways exist. It is not known if these pathways act through DIAP1.

expression of other IAPs, such as DIAP2, suppresses some of the caspase-dependent events necessary for a full apoptotic cell death phenotype. A third possibility (discussed further below) is that loss of *DIAP1* function, while sufficient to kill cells, is not sufficient to confer all aspects of apoptosis. In this scenario, proteins such as RPR, HID, or GRIM that are sufficient to trigger a full apoptotic response when overexpressed may play dual roles: inhibiting IAP function and, in addition, activating other apoptotic pathways (Figure 7).

DIAP1 Is Epistatic to *rpr*, *hid*, and *grim*

To explore further the relationship between *rpr*, *hid*, *grim*, and *DIAP1*, we made a double mutant with the H99 deficiency (which includes *rpr*, *hid*, and *grim*) and th^5. Homozygous H99 embryos essentially lack apoptosis (White et al., 1994). However, double mutants show a terminal embryonic phenotype similar to that of th^5 alone (data not shown). This, in conjunction with the fact that DIAP1 is a caspase inhibitor, argues against models in which DIAP1's sole antiapoptotic role is to bind to RPR, HID, and GRIM, thereby suppressing death pathways they activate, since in this scenario, the double mutant phenotype would be expected to be similar to that of the H99 mutant alone. Instead, our observations are consistent with models in which DIAP1 has an important antiapoptotic function as a caspase inhibitor and RPR, HID, and GRIM function, at least in part, through DIAP1 to promote apoptosis (Figure 7).

DIAP1 may, however, have antiapoptotic functions in addition to caspase inhibition. IAPs in insects and mammals have been shown to bind a number of different proteins through the BIRs in addition to caspases (reviewed in LaCasse et al., 1998). An attractive hypothesis is that some of these proteins have proapoptotic functions that do not involve disrupting IAP–caspase interactions and that death-preventing IAPs are able to suppress apoptosis induced by their expression by binding and sequestering them, preventing access to their targets. Candidates for such proteins in *Drosophila* are RPR, HID, GRIM, and DOOM (Harvey et al., 1997), as well as uncharacterized molecules that mediate normally occurring apoptotic cell death that occurs independently of expression of genes in the H99 interval (White et al., 1994; Foley and Cooley, 1998; Figure 7). DIAP1, and by extension other IAPs, may function to block death at multiple steps: at an upstream point, free DIAP1 may titrate apoptosis inducers away from their targets, DIAP1–caspase complexes and components of other effector pathways, while at a downstream point it inhibits caspase activation or activity induced by these proteins (Figure 7).

Concluding Remarks

IAPs are the only cellular caspase inhibitors identified to date. We showed that RPR, GRIM, HID, and HID fragments sufficient to cause the death of insect cells block DIAP1's ability to inhibit caspase activity. These observations provide a mechanism for RPR, HID, and GRIM action and define a novel point at which caspase activity can be regulated. The finding that the *DIAP1* loss-of-function phenotype involves cell death associated with increased caspase activity strongly suggests that the interactions we described between RPR, HID, GRIM, DIAP1, and caspases are physiologically important. Since most mammalian cells constitutively express caspases sufficient to carry out cell death (Weil et al., 1996), the mechanism of cell death activation defined by these proteins may be quite general. A prediction of our model of RPR, HID, and GRIM function is that their ability to kill will depend on the status of a cell's caspases. In cells in which caspases are activated or spontaneously undergoing autoactivation at some level, their expression may be sufficient to kill. However, in other cells in which caspase activity is either absent or more tightly regulated, they may function primarily to create a permissive condition for caspase-dependent cell death. Thus, just as IAPs in their role as caspase inhibitors may function as cellular buffers that create a requirement for a certain level of caspase activation in order to induce apoptosis, so RPR-, HID-, and GRIM-like proteins may function to titrate this buffering activity so that cells are more or less sensitive to caspase-dependent death signals.

Experimental Procedures

Yeast Strain Constructions

All yeast strains used in this study are in the W303α background (*MAT*α, *can1-100*, *leu2-3* and *-112*, *his3-11* and *-15*, *trp1-1*, *ura3-1*, *ade2-1*). Construction of pGALL-(*HIS3*), pGALL-(*LEU2*), and pGALL-DCP-1 was described previously (Hawkins et al., 1999). The p10 and prodomain-p20 fragments of drICE were amplified by PCR and inserted in tandem into pGALL-(*LEU2*) to make pGALL-rev-drICE. pAdh-(*TRP1*) was made by subcloning the promoter-terminator region from pHybZeo (Invitrogen) into pRS314. pCUP1-(*TRP1*) was constructed by replacing the GAL1 promoter of pGALL-(*TRP1*) (Hawkins et al., 1999) with the CUP1 promoter. The DIAP1 coding region was inserted into pAdh-(*TRP1*) and pCUP1-(*TRP1*) to generate pAdh-DIAP1 and pCUP-DIAP1. The HID coding region was amplified by PCR using primers that appended a C-terminal double

polyoma epitope tag and was inserted into pGALL-(*HIS3*) to generate pGALL-HID. pGALL-HID was digested with XhoI and religated to make pGALL-HIDΔ(38–335). C-terminally polyoma-tagged versions of HID initiating at codon 37 [HIDΔ(1–36)] and HID lacking the first 335 amino acids [HIDΔ(1–335)] were amplified by PCR and inserted into pGALL-(*HIS3*). The coding regions of RPR and GRIM were amplified by PCR and inserted into pGALL-(*HIS3*) to generate pGALL-RPR and pGALL-GRIM.

Cell Death Assays

Overexpression of active caspases in yeast results in cell death that is inhibited by coexpression of caspase inhibitors (Hawkins et al., 1999; Kang et al., 1999). Because expression of RPR, HID, or GRIM alone has no effect on yeast growth (below), we infer that the yeast growth suppression seen in cells that express caspases, DIAP1 and RPR, HID, or GRIM is due to cell death. To assay caspase-dependent cell death and protection by inhibitors, exponentially growing cultures of individual W303α transformants containing the relevant constructs were serially diluted 10-fold and spotted onto 2% glucose selective medium plates or 2% galactose and 1% raffinose (gal/raf)–inducing selective medium plates. Plates were incubated at 25°C for 12 hr and then at 30°C and photographed after 2 (glucose) or 3–5 (gal/raf) days.

Expression and Purification of Recombinant *Drosophila* IAPs, Caspases, and HID

DCP-1^{31}-His_6 (DCP-1-His6) was prepared as described previously (Hawkins et al., 1999) and diluted into buffer A (50 mM HEPES [pH 7.5], 100 mM NaCl, 1 mM EDTA, 0.1% CHAPS, 10% sucrose, 5 mM DTT). The DIAP1 coding region was amplified by PCR using primers that generated an N-terminal TEV protease recognition site (ENLYFQG) and was introduced into the glutathione S-transferase (GST) expression vector pGEX4T-1 (Amersham Pharmacia). The GST-TEV-DIAP1 fusion protein was expressed in *Escherichia coli* strain BL21(DE3)pLysS and was affinity purified on glutathione–Sepharose. The bound fusion protein was cleaved with TEV protease in buffer A. The coding region of HID was introduced into pET23a(+) (Novagen), generating a HID-His6 fusion. A similar procedure was used to generate a version of HID initiating at codon 37 [HIDΔ(1–36)-His6]. The first 37 amino acids of HID and the coding region of GST were PCR amplified and introduced in tandem into pET23a(+) to generate HID(1–37)GST-His6. GST was introduced into pET23a(+) to generate GST-His6. These vectors were introduced into BL21(DE3)pLysS, protein expressed, and affinity purified from the soluble fraction using ProBond resin (Invitrogen). Proteins were eluted and stored at −80°C in buffer D (50 mM HEPES [pH 8.0], 100 mM NaCl, 1 mM EDTA, 0.1% CHAPS, 10% sucrose, 20 mM 2-mercaptoethanol, 1% Triton X-100, 20% glycerol, 0.55 M imidazole).

A caspase cleavage site (DQVD) at residue 20 of DIAP1 (S. L. W., unpublished) was altered to DQVE in GST-mycDIAP1 (Hawkins et al., 1999), generating GST-DIAP1. GST and GST-DIAP1 were purified on glutathione–Sepharose beads. The mutated myc-DIAP1 coding sequence was inserted into pMAL-c2 (New England Biolabs), generating MBP-DIAP1. MBP and MBP-DIAP1 were purified on amylose resin.

In Vitro Protease Assays

HID's ability to inhibit DIAP1 was determined from caspase activity assay progress curves in which the release of 7-amino-4-trifluoromethyl-coumarin (AFC) from the synthetic substrate Ac-DEVD-AFC (100 μM) by DCP-1-His6 (0.2 nM) was measured in the presence of GST (0.2 μM) or DIAP1 (0.1 μM) and HID-His6 (0.44 μM), HIDΔ(1–36)-His6 (0.44 μM), or GST (0.77 μM). Caspase activity assays were performed in triplicate and prepared as follows. Two microliters DCP-1-His6 was incubated with 5 μl DIAP1 or GST for 5 min at 25°C. Seventy-one microliters buffer X (70.4 mM HEPES [pH 7.5], 140.8 mM NaCl, 1.4 mM EDTA, 0.14% CHAPS, 14.1% sucrose, 3.5 mM DTT, 5.6 % glycerol, and 0.7% Triton X-100) and 20 μl HID-His6, HIDΔ(1–36)-His6, or GST-His6 was subsequently added and the samples further incubated 23 min. After addition of 2 μl 5 mM Ac-DEVD-AFC in DMSO to each sample, caspase activities were assayed at 27°C using a fluorometric plate reader (Molecular Devices, fmax) in the kinetic mode with excitation and emission wavelengths of 405 and 510 nm, respectively. HID(1–37)GST-His6 activity, used at a concentration of 1.6 μM, was tested in a similar manner.

Caspase activity of embryos was monitored as follows. Zero to two-hr-old embryos were collected and aged for 3 hr at 25°C. Embryos were dechorionated with 50% bleach, rinsed, suspended in an equal volume of buffer E (buffer A containing 0.5% Triton X-100 and 4% glycerol), and homogenized. One microliter of this extract (approximately 10 mg/ml) was diluted into 100 μl of buffer E in the presence of 100 μM Ac-DEVD-AFC. Assays were performed in triplicate with freshly prepared extracts.

Protein Binding Assays

Purified recombinant proteins (150 ng each) were incubated with either GST beads, MBP beads, GST-DIAP1 beads, or MBP-DIAP1 beads (200 ng) for 30 min on a rotator at 25°C in buffer C (100 mM HEPES [pH 7.5], 200 mM NaCl, 2 mM EDTA, 0.2% CHAPS, 20% sucrose, 40 mM 2-mercaptoethanol, 1% Triton X-100, 8% glycerol). Beads were then washed three times for 5 min with 1 ml buffer D lacking imidazole. Bead–protein complexes were subjected to 15% SDS-PAGE and immunoblotting. Proteins were detected with an anti-His antibody (Qiagen) and HRP-conjugated secondary antibodies followed by ECL (Amersham).

HID-DCP-1 Competition Assay

MBP or MBP-DIAP1 beads (0.5 μg) were mixed with 1, 5, or 20 μg GST-His6 or HID(1–37)GST-His6 for 1 hr at 4°C in buffer A. Five micrograms of DCP-1-His6 was added and the samples further incubated for 10 min. After extensive washing, the bead–protein complexes were subjected to 15% SDS-PAGE and immunoblotting. Proteins were detected with an anti-His antibody and HRP-conjugated secondary antibodies followed by ECL.

Drosophila Strains

A w^- Oregon R strain was used as wild type. The deficiency *Df(3L)brm11* (72A3–4; 72D1–5) uncovers *DIAP1*. *DIAP1* mutants, alleles of the *th* locus, and *Df(3L)brm11* were kept as balanced stocks over a version of the TM3 balancer that carries an ftz::lacZ transgene (TM3[ftz::lacZ]). th^5 is a loss-of-function mutation in *DIAP1*, since *Df(3L)brm11* shows a GMR-*rpr* enhancer phenotype similar to that of th^5 (Hay et al., 1995), and the embryonic lethal phenotype of th^5/*Df(3L)brm11* (this work, data not shown) is similar to that of th^5/th^5. By these same criteria, th^6 is a much weaker allele.

Cell Death Assays and Microscopy

Embryos were collected on yeasted apple juice plates. For observation of living embryos, syncytial blastoderm stages were selected under halocarbon oil 27 (Sigma) and mounted individually on a slide using 10 mm coverslips. Images were taken on a Zeiss Axiophot from sets of six embryos per experiment every 15 min at 25°C.

For scanning electron microscopy, staged collections of embryos were processed for staining with anti-β-galactosidase (β-gal) antibodies (Cappel) as described elsewhere (Müller and Wieschaus, 1996). Homozygotes were isolated under the dissecting scope; the remaining embryos served as controls. The embryos were then processed for scanning electron microscopy as described in Müller and Wieschaus (1996). Samples were viewed under a Hitachi S800 SEM.

TUNEL labeling was performed using an in situ cell death detection kit (Roche). Embryos were fixed as described above, rinsed in PTX (PBS, 0.5% Triton X-100), and immunolabeled with antibodies against β-gal (Cappel) and Cy3-conjugated goat anti-rabbit (Jackson) secondary antibodies. Embryos were then incubated in 100 mM sodium-citrate, 0.1% Triton X-100 at 65°C for 30 min, followed by rinsing twice in PTX and twice in TUNEL dilution buffer (Roche). Embryos incubated in TUNEL assay buffer (Roche; 30 min to 2 hr) were supplemented with TUNEL enzyme (Roche) and incubated a further 2 to 3 hr at 37°C. Embryos were rinsed in PTX and mounted in MOWIOL (Polysciences) containing DABCO (Sigma). Images were taken on a Leica TSC-NT confocal microscope. A range of 50 μm in depth was scanned in 16 optical sections and projected into one focal plane using the TCS-NT software.

Acridine orange staining was carried out as described in Hay et al. (1994). Confocal and Nomarksi images were taken on the confocal microscope.

Acknowledgments

We thank R. Deshaies and members of his lab for advice with protein binding and yeast experiments and H. Schwarz and J. Berger (MPI Tübingen, Germany) for the use of their SEM. We also thank R. Deshaies, P. Sternberg, and M. Guo for comments on the manuscript. H.-A. J. M. thanks E. Wieschaus for discussions. C. J. H. is supported by a Human Frontiers postdoctoral fellowship. B. A. H. is a Searle Scholor. This work was supported by a DFG research fellowship (MU1168/1-1) to H.-A. J. M. and by grants to B. A. H. from the Gustavus and Louise Pfeiffer Research Foundation, a Burroughs Wellcome Fund New Investigator Award in the Pharmacological Sciences, the Ellison Medical Foundation, and National Institutes of Health Grant GM057422-01.

Received May 28, 1999; revised July 13, 1999.

References

Abrams, J.M., White, K., Fessler, L.I., and Steller, H. (1993). Programmed cell death during *Drosophila* embryogenesis. Development *117*, 29–43.

Alnemri, E.S., Livingston, D.J., Nicholson, D.W., Salvesen, G., Thornberry, N.A., Wong, W.W., and Yuan, J. (1996). Human ICE/CED3 protease nomenclature. Cell *87*, 171.

Avdonin, V., Kasuya, J., Ciorba, M.A., Kaplan, B., Hoshi, T., and Iverson, L. (1998). Apoptotic proteins Reaper and Grim induce stable inactivation in voltage gated K^+ channels. Proc. Natl. Acad. Sci. USA *95*, 11703–11708.

Bergmann, A., Agapite, J., McCall, K., and Steller, S. (1998). The *Drosophila* gene *hid* is a direct molecular target of Ras-dependent survival signaling. Cell *95*, 331–341.

Birnbaum, M.J., Clem, R.J., and Miller, L.K. (1994). An apoptosis-inhibiting gene from a nuclear polyhedrosis virus encoding a peptide with Cys/His sequence motifs. J. Virol. *68*, 2521–2528.

Cavaliere, V., Taddei, C., and Gargiulo, G. (1998). Apoptosis of nurse cells at the late stages of oogenesis of *Drosophila melanogaster*. Dev. Genes Evol. *208*, 106–112.

Chen, P., Nordstrom, W., Gish, B., and Abrams, J.M. (1996). *grim*, a novel cell death gene in *Drosophila*. Genes Dev. *10*, 1773–1782.

Chen, P., Rodriguez, A., Erskine, R., Thach, T., and Abrams, J.M. (1998). *Dredd*, a novel effector of the apoptosis activators *reaper*, *grim* and *hid* in *Drosophila*. Dev. Biol. *201*, 202–216.

Crook, N.E., Clem, R.J., and Miller, L.K. (1993). An apoptosis-inhibiting baculovirus gene with a zinc finger-like motif. J. Virol. *67*, 2168–2174.

Cryns, V., and Yuan, J. (1998). Proteases to die for. Genes Dev. *12*, 1551–1570.

Deveraux, Q.L., and Reed, J.C. (1999). IAP family proteins—suppressors of apoptosis. Genes Dev. *13*, 239–252.

Deveraux, Q.L., Takahashi, R., Salvesen, G.S., and Reed, J.C. (1997). X-linked IAP is a direct inhibitor of cell-death proteases. Nature *388*, 300–304.

Deveraux, Q.L., Roy, N., Stennicke, H.R., Arsdale, T.V., Zhou, Q., Srinivasula, S.M., Alnemri, E.S., Salvesen, G.S., and Reed, J.C. (1998). IAPs block apoptotic events induced by caspase-8 and cytochrome c by direct inhibition of distinct caspases. EMBO J. *17*, 2215–2223.

Dorstyn, L., Colussi, P.A., Quinn, L.M., Richardson, H., and Kumar, S. (1999). DRONC, an ecdysone-inducible *Drosophila* caspase. Proc. Natl. Acad. Sci. USA *96*, 4307–4312.

Duckett, C.S., Nava, V.E., Gedrich, R.W., Clem, R.J., Van Dongen, J.L., Gilfillan, C., Shiels, H., Hardwick, J.M., and Thompson, C.B. (1996). A conserved family of cellular genes related to the baculovirus iap gene and encoding apoptosis inhibitors. EMBO J. *15*, 2685–2694.

Evans, E.K., Kuwana, T., Strum, S.L., Smith, J.J., Newmeyer, D.D., and Kornbluth, S. (1997). Reaper-induced apoptosis in a vertebrate system. EMBO J. *16*, 7372–7381.

Foley, K., and Cooley, L. (1998). Apoptosis in late stage *Drosophila* nurse cells does not require genes within the H99 deficiency. Development *125*, 1075–1082.

Fraser, A.G., and Evan, G.I. (1997). Identification of a *Drosophila melanogaster* ICE/CED-3-related protease, drICE. EMBO J. *16*, 2805–2813.

Fraser, A.G., McCarthy, N.J., and Evan, G.I. (1997). drICE is an essential caspase required for apoptotic activity in *Drosophila* cells. EMBO J. *20*, 6192–6199.

Grether, M.E., Abrams, J.M., Agapite, J., White, K., and Steller, H. (1995). The *head involution defective* gene of *Drosophila melanogaster* functions in programmed cell death. Genes Dev. *9*, 1694–1708.

Harvey, A.J., Bidwai, A.P., and Miller, L.K. (1997). Doom, a product of the *Drosophila* mod(mdg4) gene, induces apoptosis and binds to baculovirus inhibitor-of-apoptosis proteins. Mol. Cell. Biol. *17*, 2835–2843.

Hawkins, C.J., Wang, S.L., and Hay, B.A. (1999). A cloning method to identify caspases and their regulators in yeast: identification of *Drosophila* IAP1 as an inhibitor of the *Drosophila* caspase DCP-1. Proc. Natl. Acad. Sci. USA *96*, 2885–2890.

Hay, B.A., Wolff, T., and Rubin, G.M. (1994). Expression of baculovirus p35 prevents cell death in *Drosophila*. Development *120*, 2121–2129.

Hay, B.A., Wassarman, D.A., and Rubin, G.M. (1995). *Drosophila* homologs of baculovirus inhibitor of apoptosis proteins function to block cell death. Cell *83*, 1253–1262.

Inohara, N., Koseki, T., Hu, Y.M., Chen, S., and Nunez, G. (1997). CLARP, a death effector domain-containing protein interacts with caspase-8 and regulates apoptosis. Proc. Natl. Acad. Sci. USA *94*, 10717–10722.

Kaiser, W.J., Vucic, D., and Miller, L.K. (1998). The *Drosophila* inhibitor of apoptosis D-IAP1 suppresses cell death induced by the caspase drICE. FEBS Lett. *440*, 243–248.

Kang, J.K., Schaber, M.D., Srinivasula, S.M., Alnemri, E.S., Litwack, G., Hall, D.J., and Bjornsti, M.A. (1999). Cascades of mammalian caspase activation in the yeast *Saccharomyces cerevisiae*. J. Biol. Chem. *274*, 3189–3198.

LaCasse, E.C., Baird, S., Korneluk, R.G., and MacKenzie, A.E. (1998). The inhibitors of apoptosis (IAPs) and their emerging role in cancer. Oncogene *17*, 3247–3259.

McCall, K., and Steller, H. (1998). Requirement for DCP-1 caspase during *Drosophila* oogenesis. Science *279*, 230–234.

Müller, H.A., and Wieschaus, E. (1996). *armadillo*, *bazooka*, and *stardust* are critical for early stages in formation of the zonula adherens and maintenance of the polarized blastoderm epithelium in *Drosophila*. J. Cell Biol. *134*, 149–163.

Nicholson, D.W., and Thornberry, N. (1997). Caspases: killer proteases. Trends Biochem. Sci. *22*, 299–306.

Raff, M.C. (1992). Social controls on cell survival and cell death. Nature *356*, 397–400.

Roy, N., Deveraux, Q.L., Takahashi, R., Salvesen, G.S., and Reed, J.C. (1997). The c-IAP-1 and c-IAP-2 proteins are direct inhibitors of specific caspases. EMBO J. *16*, 6914–6925.

Salvesen, G.S., and Dixit, V.M. (1997). Caspases: intracellular signaling by proteolysis. Cell *91*, 443–446.

Song, Z.W., McCall, K., and Steller, H. (1997). DCP-1, a *Drosophila* cell death protease essential for development. Science *275*, 536–540.

Srinivasula, S.M., Ahmed, M., MacFarlane, A.M., Luo, Z.W., Fernandes-Alnemri, T., and Alnemri, E.S. (1998). Generation of constitutively active recombinant caspases-3 and -6 by rearrangement of their subunits. J. Biol. Chem. *273*, 10107–10111.

Takahashi, R., Deveraux, Q.L., Tamm, I., Welsh, K., Assa-Munt, N., Salvesen G., and Reed, J.C. (1998). A single BIR domain of XIAP sufficient for inhibiting caspases. J. Biol. Chem. *273*, 7787–7790.

Thornberry, N.A., and Lazebnik, Y. (1998). Caspases: enemies within. Science *281*, 1312–1316.

Thress, K., Henzel, W., Shillinglaw, W., and Kornbluth, S. (1998). Scythe: a novel reaper-binding apoptotic regulator. EMBO J. *17*, 6135–6143.

Uren, A.G., Pakusch, M., Hawkins, C.J., Puls, K.L., and Vaux, D.L. (1996). Cloning and expression of apoptosis inhibitory protein homologs that function to inhibit apoptosis and/or bind tumor necrosis factor receptor-associated factors. Proc. Natl. Acad. Sci. USA *93*, 4974–4978.

Uren, A.G., Coulson, E.J., and Vaux, D.L. (1998). Conservation of baculovirus inhibitor of apoptosis repeat proteins (BIRPs) in viruses, nematodes, vertebrates and yeasts. Trends Biochem. Sci. *23*, 159–162.

Vucic, D., Kaiser, W.J., Harvey, A.J., and Miller, L.K. (1997). Inhibition of Reaper-induced apoptosis by interaction with inhibitor of apoptosis proteins (IAPs). Proc. Natl. Acad. Sci. USA *94*, 10183–10188.

Vucic, D., Kaiser, W.J., and Miller, L.K. (1998). Inhibitor of apoptosis proteins physically interact with and block apoptosis induced by *Drosophila* proteins HID and GRIM. Mol. Cell. Biol. *17*, 667–676.

Weil, M., Jacobson, M.D., Coles, H.S.R., Davies, R.L., Gardner, R.L., Raff, K.D., and Raff, M.C. (1996). Constitutive expression of the machinery for programmed cell death. J. Cell Biol. *133*, 1053–1059.

White, K., Grether, M.E., Abrams, J.M., Young, L., Farrell, K., and Steller, H. (1994). Genetic control of programmed cell death in *Drosophila*. Science *264*, 677–683.

White, K., Tahaoglu, E., and Steller, H. (1996). Cell killing by the *Drosophila* gene *reaper*. Science *271*, 805–807.

Wing, J.P., Zhou, L., Schwartz, L.M., and Nambu, J.R. (1998). Distinct cell killing properties of the *Drosophila reaper*, *head involution defective*, and *grim* genes. Cell Death Differ. *5*, 930–939.

Wyllie, A.H., Kerr, J.F.R., and Currie, A.R. (1980). Cell death: the significance of apoptosis. Int. Rev. Cytol. *68*, 251–303.

Zhou, L., Schnitzler, A., Agapite, J., Schwartz, L.M., Steller, H., and Nambu, J.R. (1997). Cooperative functions of the *reaper* and *head involution defective* genes in the programmed cell death of *Drosophila* central nervous system midline cells. Proc. Natl. Acad. Sci. USA *94*, 5131–5136.